

SHORT COMMUNICATION

Functional analyses and molecular modeling of two *c-Kit* mutations responsible for imatinib secondary resistance in GIST patientsE Tamborini^{1,7}, S Pricl^{2,7}, T Negri¹, MS Lagonigro¹, F Miselli¹, A Greco³, A Gronchi⁴, PG Casali⁵, M Ferrone², M Fermeglia², A Carbone¹, MA Pierotti^{3,6,8} and S Pilotti^{1,8}¹Experimental Molecular Pathology, Department of Pathology, Istituto Nazionale per lo Studio e la Cura dei Tumori, Milan, Italy;²Molecular Simulation Engineering Laboratory, DICAMP University of Trieste, Trieste, Italy; ³Department of Experimental Oncology, Istituto Nazionale per lo Studio e la Cura dei Tumori, Milan, Italy; ⁴Department of Surgery, Istituto Nazionale per lo Studio e la Cura dei Tumori, Milan, Italy; ⁵Department of Clinical Oncology, Istituto Nazionale per lo Studio e la Cura dei Tumori, Milan, Italy and ⁶IFOM, FIRC Institute of Molecular Oncology, Milan, Italy

Imatinib-acquired resistance related to the presence of secondary point mutations has become a frequent event in gastrointestinal stromal tumors. Here, transient transfection experiments with plasmids carrying two different KIT-acquired point mutations were performed along with immunoprecipitation of total protein extracts, derived from imatinib-treated and untreated cells. The molecular mechanics/Poisson Boltzmann surface area computational techniques were applied to study the interactions of the wild-type and mutated receptors with imatinib at the molecular level. Biochemical analyses showed KIT phosphorylation in cells transfected with vectors carrying the specific mutant genes. Imatinib treatment demonstrated that T670I was insensitive to the drug at all the applied concentrations, whereas V654A was inhibited by 6 μ M of imatinib. The modeling of the mutated receptors revealed that both substitutions affect imatinib-binding site, but to a different extent: T670I substantially modifies the binding pocket, whereas V654A induces only relatively confined structural changes. We demonstrated that T670I and V654A cause indeed imatinib-acquired resistance and that the former is more resistant to imatinib than the latter. The application of molecular simulations allowed us to quantify the interactions between the mutated receptors and imatinib, and to propose a molecular rationale for this type of drug resistance.

Oncogene advance online publication, 5 June 2006; doi:10.1038/sj.onc.1209639

Keywords: imatinib secondary resistance; gastrointestinal stromal tumors (GIST); molecular modeling

Gastrointestinal stromal tumors (GIST) are the most common mesenchymal malignancies of the gastrointestinal tract and are characterized by the presence of constitutively activated KIT (CD117) or PDGFRA receptors. In both the receptors, the mechanism responsible for kinase activation is mainly represented by gain-of-function mutations, which always affect specific exons (Corless *et al.*, 2004). To date, several types of mutations have been described and the main mutational ‘hot spot’ is represented by *c-Kit* exon 11 (Corless *et al.*, 2002; Heinrich *et al.*, 2003).

Imatinib mesylate (Glivec™, Novartis, Basel, Switzerland) is an inhibitor of a number of tyrosine kinases including the intracellular kinase ABL, the growth factor receptors KIT, PDGFR β and α and ARG and their oncogenic activated forms. Imatinib competes with ATP for ATP-binding site of the kinase preventing the downstream signaling.

Recently, GIST cases showing acquired resistance to imatinib, that is, tumoral growth after an initial response, have been reported and molecularly analysed (Chen *et al.*, 2004; Tamborini *et al.*, 2004, 2005; Antonescu *et al.*, 2005; Debiec-Rychter *et al.*, 2005; Wardelmann *et al.*, 2005). Although several mechanisms have been proposed to be responsible for this phenomenon, including *KIT* gene amplification, the emergence of additional point mutations appears to be the most frequent event. This suggests that imatinib secondary resistance in GIST may be an ‘in expansion phenomenon’ not yet fully investigated in terms of temporal development of the disease.

The secondary point mutations till now described always involve the kinase domain of the receptor and have been described in exons 13, 14 and 17 of *c-Kit* gene and in exon 18 of *PDGFRA* gene (Chen *et al.*, 2004; Tamborini *et al.*, 2004, 2005; Antonescu *et al.*, 2005; Debiec-Rychter *et al.*, 2005; Wardelmann *et al.*, 2005). Their presence in the ATP pocket of the kinase suggests that imatinib is not able to inhibit the receptor efficiently, most likely because of a different tridimensional proteic structure of the ATP pocket induced by these additional mutations.

Correspondence: Dr S Pilotti, Unit of Experimental Molecular Pathology, Istituto Nazionale per lo Studio e la Cura dei Tumori, Via G Venezian 1, Milan 20133, Italy.

E-mail: silvana.pilotti@istitutotumori.mi.it

⁷These authors contributed equally to this work.

⁸Senior co-authors.

Received 9 January 2006; revised 21 March 2006; accepted 23 March 2006

In this work, by means of biochemical assay on cells transfected with KIT mutants and treated with different doses of imatinib, we have demonstrated that two KIT mutations detected in three GIST patients with acquired resistance to imatinib are actually responsible for this phenomenon. The coupled molecular modeling simulations on the same mutated receptors allowed us to quantify the interactions between the mutated receptors and the drug, thus providing a molecular rationale for the modulation of the differences in drug resistance.

A series of patients surgically treated at the Istituto Nazionale per lo Studio e la Cura dei Tumori-Milan, all showing clinical/radiological evidence of progressing disease during imatinib treatment after an initial response, were investigated for the presence of *KIT* and *PDGFRA* gene mutations. A written informed consent was obtained from each subject.

The sequencing of the whole coding sequence of *KIT* revealed activating mutations in exon 11 in all of the patients. In three patients, characterized by the following exon 11 mutations ($\Delta 557-558$ in patient 1, V559A in patient 2 and W557G in patient 3), two different adjunctive point mutations in *KIT* gene were detected: one (in patient 1) (Tamborini *et al.*, 2004) in exon 14 responsible for T670I substitution, threonine versus isoleucine, and one (in two different patients, 2 and 3, respectively) in exon 13 causing the V654A substitution, valine versus alanine (Tamborini *et al.*, 2005). None of the patients revealed mutations affecting *PDGFRA* gene.

The morphological and immunohistochemical analysis of the imatinib-insensitive tumors revealed highly cellulated tumoral samples with strong cytoplasmic CD117 positivity. Immunoprecipitation and Western blot experiments showed highly expressed and phosphorylated KIT receptors despite all of these patients being treated with imatinib (Tamborini *et al.*, 2004, and data not shown).

Imatinib mesylate activity on KIT mutants

In order to verify whether the amino-acidic changes caused by exons 14 and 13 mutations were actually responsible for the acquired resistance to imatinib, the T670I and the V654A mutations were introduced into the wild-type *c-Kit* cDNA contained in an expression vector. The resulting constructs, KIT/T670I and KIT/V654A, were transiently expressed into COS1 cells. As positive control in the experiments, the KIT/ $\Delta 559$ mutant, carrying the deletion of residue 559 and previously shown to respond to imatinib (Tamborini *et al.*, 2004), was used.

Based on antiphosphotyrosine immunoblot analysis with cells treated with three different doses of the drug, KIT/T670I and KIT/V654A were clearly resistant to imatinib compared to the KIT/ $\Delta 559$ imatinib-sensitive mutation. KIT/T670I appeared to be phosphorylated and thus insensitive to the drug at all the doses used, whereas KIT/V654A appeared to be totally inhibited at 6 μM of imatinib (Figure 1a, upper panel).

As in all the patients, in whom these amino-acidic substitutions were present, the corresponding DNA mutations were on the same allele carrying also the activating exon 11 *KIT* mutation, we investigated the effect of their presence on an activated KIT receptor. Through a specific PCR reaction, we obtained a DNA fragment spanning a *KIT* cDNA region from exon 11 to 14. We subcloned it into pGEM vector, and the sequencing of several colonies revealed that on the same DNA fragment, both the mutations (exon 11 plus exon 13 or 14) were present.

We introduced therefore the T670I and the V654A mutations into the activated KIT/ $\Delta 559$ mutant, previously shown to be inhibited by imatinib. The resulting KIT/ $\Delta 559$ /T670I and KIT/ $\Delta 559$ /V654A mutants were transiently expressed in COS1 cells. Western blot analysis showed that KIT/ $\Delta 559$ /T670I was resistant to imatinib at all the concentrations, whereas KIT/ $\Delta 559$ /V654A appeared to be reduced at 3 μM and inhibited at the dose of 6 μM of imatinib (Figure 1b, lower panel).

Molecular modeling

Mutating T into I at position 670 in the ATP-binding site of the KIT kinase domain results in a calculated $\Delta\Delta G_{\text{bind}}$ for imatinib equal to -3.84 kcal/mol (Table 1). Both nonbonded interaction components of the free energy of binding strongly decrease in the presence of the mutated isoform ($\Delta\Delta E_{\text{MM}} = -5.87$ kcal/mol; Table 1). This markedly decreased affinity for this mutant with respect to imatinib might be ascribed to the molecular dimensions of the inhibitor, which are too big to result in a snug fit within the pocket formed at the N- and C-lobe interface of the inactive structure of the kinase. Indeed, the phenyl ring of imatinib packs too tightly between the aliphatic chains of D810, E640 and L644, whereas the piperazine ring makes no specific interactions with the protein and fits in a shallow pocket bounded by V643, C788, I789, H790, R791 and D810 (Figure 2a). As seen for the analogous mutation T315I in the ABL kinase domain (Priest *et al.*, 2005), in a sort of a domino effect, the substitution of this single residue in this position induces several, sometimes substantial, modifications in the conformation of other residues, both belonging to the binding site and the surrounding areas, as a direct consequence of the different position assumed by imatinib in the binding site. The topical, stabilizing hydrogen bond between the aminopyridine nitrogen of imatinib and the side chain O γ 1 atom of the gatekeeper residue T670 does no longer exist, and is not replaced by any similar, favorable interaction (Figure 2b and c). Moreover, the greater molecular volume of isoleucine (I) side chain with respect to threonine (T) (73.0 versus 48.6 \AA^3 , respectively) induces imatinib to assume a slightly modified position within the pocket (Figure 2b and c), to alleviate sterical unfavorable interferences. From an electrostatic viewpoint, the T670I mutant protein is further penalized, as a nonpolar moiety, such as the isoleucine side chain, is surrounded

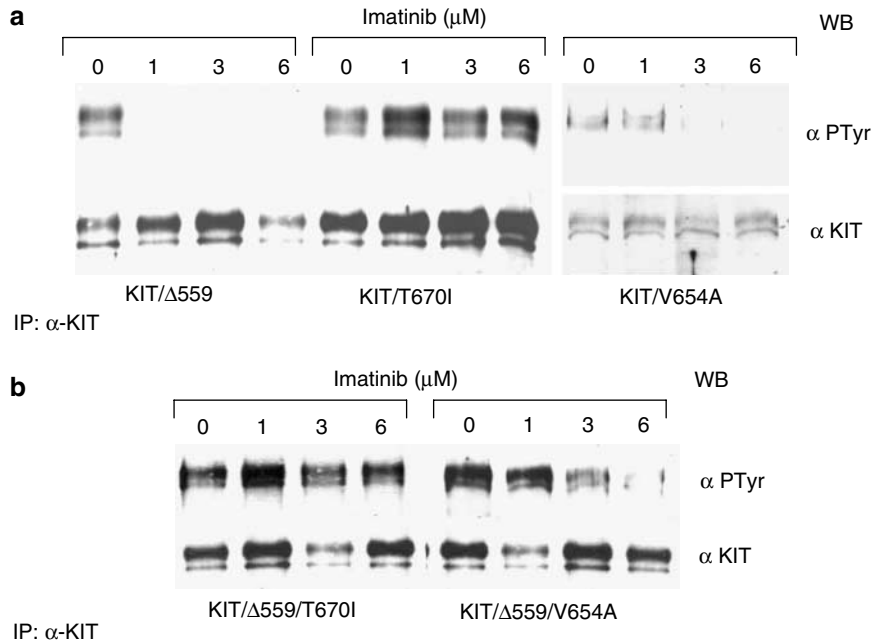


Figure 1 Imatinib mesylate activity on KIT mutants. **(a)** COS1 cells were transiently transfected with the *c-Kit* constructs (KIT/T670I and KIT/V654A). *c-Kit* mutants were constructed by means of site-directed mutagenesis using the Promega kit, and an expression vector carrying a wild-type *c-Kit* gene (kindly provided by Dr Yarden) was used as template. The mutant Δ559 was obtained by deleting base pairs 1696–1698 (GTT) in exon 11 of the wild-type gene; the T670I mutant was obtained by substituting the base C 2030 with T in exon 14; and the V654A mutant was obtained by substituting the base T1982 with a C in exon 13. All the plasmids were sequenced in order to verify the success of mutagenesis experiments. The transfected cells were incubated with imatinib at the indicated doses for 8 h. Protein extracts from the transfected cells were obtained by means of homogenization at 4°C in lysis buffer (50 mM Hepes, 150 mM NaCl, 10% glycerol, 1% Triton X-100, 1.5 mM MgCl₂, 1 mM EGTA, 10 mM Na₄P₂O₇ and 100 mM NaF) supplemented with protease and phosphatase inhibitors (Protease Inhibitor Cocktail, Phosphatase Inhibitor Cocktail 2, phenylmethylsulfonyl-fluoride, Sigma, St Louis, MO, USA). After lysing by means of frequent vortexing, the protein lysates were cleared by means of centrifugation at 13 000 r.p.m. at 4°C for 30 min, and quantitated using the Bio-Rad protein assay (Bio-Rad, Hercules, CA, USA). Total protein extracts (1 mg) were immunoprecipitated using 360 ng of Ab-3 (K45) (Neomarkers, Fremont, CA, USA) monoclonal antibody directed against KIT receptor as described previously (Tamborini *et al.*, 2004); the positive control was 500 μg of Δ559 cell line lysate. Both the mature (145 kDa) and partially glycosylated (125 kDa) forms of KIT receptor were detected. **(b)** Same as panel A, but using the KIT/Δ559/T670I and KIT/Δ559/V654A mutants. T670I and V654A mutations were introduced into Δ559/KIT mutant. In these experiments, 500 μg of total protein extract was immunoprecipitated and used for Western blot analysis. Both KIT receptor isoforms (mature and partially glycosylated forms) were detected.

Table 1 Calculated free energy of binding ΔG_{bind} (kcal/mol) and energy contributions to ΔG_{bind} (kcal/mol) of wild-type, T670I and V654A mutant c-Kit kinase domains and Imatinib

Contribution	Wild type	T670I	V654A
ΔE_{vdW}	-72.10	-68.27	-71.02
ΔE_{EL}	-56.01	-53.97	-55.82
ΔE_{MM}	-128.11	-122.24	-126.84
ΔG_{PB}	107.21	105.03	107.44
ΔG_{NP}	-6.69	-6.29	-6.33
$-T\Delta S$	17.37	17.12	17.03
ΔG_{bind}	-10.22	-6.38	-8.70
$\Delta\Delta G_{\text{bind}}$	—	-3.84	-1.52

by a strongly polar environment generated by three nitrogen atoms of imatinib (Figure 2c). The universally conserved DGF motif, fundamental for the catalytic activity, is kept in the inhibited orientation in the wild-type KIT–imatinib complex, whereas it moves toward the productive state in the mutated complex. This is caused by the deleterious readjustment of the DGF

motif, mainly owing to a steric clash of the inhibitor with the side chain of F810 (Figure 2d). Finally, the active kinase structure is characterized by a critical salt link between a conserved C-helix D640 and K623 that orients the lysine side chain for interactions with the nucleotide phosphate (Mol *et al.*, 2003). This salt link, absent in the trajectory of the wild-type KIT/imatinib, is present in the corresponding molecular dynamics (MD) simulation of the T670I mutant/imatinib complex, with an average dynamic length of 2.8 Å.

Residue V654 is in KIT kinase domain 1, and is notably conserved among other kinases such as Abl, Src, Hck, Flt3 and PDGFR. Mutating V to A at position 654 in the ATP-binding domain of the KIT results in calculated $\Delta\Delta G_{\text{bind}}$ for imatinib of -1.52 kcal/mol. Indeed, exchanging V to A decreases the degree of surface complementarity between KIT and the inhibitor, owing to the smaller A dimensions (Figure 3a and b), which account for the most part of the nonbonded interactions ($\Delta\Delta E_{\text{vdW}} = -1.08$ kcal/mol and $\Delta\Delta E_{\text{MM}} = -1.27$ kcal/mol; Table 1). In contrast to that observed for the T670I mutation, in fact, both the

electrostatic and solvation terms remain almost unaffected, as expected for a conservative substitution (Table 1). We can conclude that this decrease in the binding affinity is substantially owing to the loss of packing interaction (i.e., cavity formation) in the native state of the alanine-containing variant (Figure 3c and d). We can then estimate the destabilizing effect of cavity formation per one carbon (methyl group) atom. The V to A substitution removes two carbon atoms; the

calculated $\Delta\Delta G_{\text{bind}}$ for V654A mutant disfavors the mutant by 1.52 kcal/mol, resulting in a destabilization of approximately 0.8 kcal/mol per carbon atom upon cavity formation. This estimate is in good agreement with the results of earlier experimental studies (Kellis *et al.*, 1988; Eriksson *et al.*, 1992; Pace *et al.*, 1996; Loladze *et al.*, 2002) and theoretical calculations (Nicholls *et al.*, 1991; Lee, 1993; Lazaridis *et al.*, 1995). Replacing V with A at position 654 further

Figure 2 Molecular modeling of KIT/T670I mutant. The procedure applied in this work has been described in detail in our previous work (Pricl *et al.*, 2005). Accordingly, only a brief outline of the method is reported. All simulations were carried out using the *Sander* modulus of AMBER 7.0 (Case *et al.*, 2000) and the Cornell *et al.* (1995) force field. The 1.60-Å-resolution coordinates of the kinase domain of KIT in complex with imatinib were obtained from the Brookhaven Protein Data Bank (PDB code 1T46) (Mol *et al.*, 2004), and used as the starting structure. All crystallographic water molecules were included, and the missing hydrogen atoms were added to the protein backbone and side chains with the *Parse* module of AMBER 7.0. All ionizable residues were considered in the standard ionization state at neutral pH. The missing force field parameters for the inhibitor were taken from our previous work (Pricl *et al.*, 2005). Mutations T670I and V654A were introduced into the wild-type structure of KIT/imatinib complex using the Biopolymer module of Insight II (v. 2001, Accelrys Inc., San Diego, CA, USA) by swapping the mutant residue into the specific site, according to a dedicated and well-validated procedure (Reyes and Kollman, 2000; Pricl *et al.*, 2005). To set up each resulting complex for the simulation, we adopted the following ansatz: first, each complex was immersed in a sphere of TIP3P water molecules (Jorgensen *et al.*, 1983). To achieve electroneutrality, a suitable number of counterions were added, in the positions of largest electrostatic potential, as determined by the module *Cion* within AMBER 7.0. All three systems (wild type, T670I and V654A KIT/imatinib complexes, respectively) were then minimized and equilibrated with the same protocol. Briefly, the energy of each complex was gradually minimized, followed by 40 ps of dynamics of the water molecules, to let the water relax around the solute. At the end of the relaxation process, all water molecules beyond the first hydration shell were removed. To reduce computational time to reasonable limits, all protein residues with any atom closer than 30 Å from the center of mass of the considered mutation were chosen to be flexible in the subsequent dynamic simulations. Subsequently, a spherical TIP3P water cap of radius equal to 30 Å was centered on imatinib in each corresponding complex, including the hydrating water molecules within the sphere resulting from the previous step. The new water cap was relaxed, followed by another gradual and global energy minimization of the entire system. Using separate solvent–solute Berendsen temperature coupling (Berendsen *et al.*, 1984), each system was heated up to 300 K in three stages. This gradual heating served to equilibrate the kinetic energy of the system, evenly distributing it among the many degrees of freedom. Each hydrated complex was then further equilibrated for 50 ps at 300 K, and we continued each simulation for the other 400 ps at 300 K, a time necessary for the estimation of the free energy of binding (*vide infra*). The molecular dynamics (MD) simulations were performed using an integration time step of 2 fs and by the application of the *Shake* algorithm (Ryckaert *et al.*, 1977). Long-range nonbonded interactions were truncated by using a dual cutoff of 12 and 30 Å. The simulations of the three complexes were performed on a cluster of Silicon Graphics Octane (single and dual processor R12K). All energetic analysis was carried out for only a single MD trajectory of each KIT/imatinib complex considered, with unbound protein and substrate snapshots taken from the snapshots of that trajectory. According to the so-called molecular mechanics/Poisson–Boltzmann surface area method (Gilson *et al.*, 1987), the binding free energy between imatinib and c-Kit can be calculated as follows:

$$\Delta G_{\text{bind}} = \Delta E_{\text{MM}} + \Delta G_{\text{solv}} - T\Delta S \quad (1)$$

where

$$\Delta G_{\text{solv}} = \Delta G_{\text{PB}} + \Delta G_{\text{NP}} \quad (2)$$

ΔE_{MM} denotes the sum of MM energies of the molecules, and can be further split into contributions from electrostatic (E_{EL}) and van der Waals (E_{vdW}) energies:

$$\Delta E_{\text{MM}} = \Delta E_{\text{EL}} + \Delta E_{\text{vdW}} \quad (3)$$

The terms in equation (3) were calculated by using the *Carnal* and *Anal* modules of AMBER 7.0. ΔG_{solv} (see equation (2)) represents the solvation free energy. The polar solvation process (i.e., ΔG_{PB} in equation (2)) is equivalent to the transfer of a protein from one medium with dielectric constant equal to that of the interior of the protein to another medium with dielectric constant equal to that of the exterior of the protein. This term yields a free energy because it corresponds to the work carried out to reversibly charge the solute, and it is a polarization free energy because the work goes to the polarization of the solvent. It was evaluated with the Poisson–Boltzmann (PB) approach (Srinivasan *et al.*, 1998). The nonpolar solvation contribution to solvation (i.e., ΔG_{NP} in equation (2)) includes cavity creation in water and van der Waals interactions between the modeled nonpolar protein and water molecules. This term can be imagined as transferring a nonpolar molecule with the shape of the protein from vacuum to water. It was calculated (Gilson *et al.*, 1987) as $\Delta G_{\text{NP}} = \gamma (\text{SASA}) + \beta$, in which $\gamma = 0.00542 \text{ kcal}/\text{Å}^2$, $\beta = 0.92 \text{ kcal/mol}$ and SASA is the solvent-accessible surface estimated with the MSMS program (Sanner *et al.*, 1996). Finally, the normal-mode analysis approach was followed to estimate the last parameter, that is, the change in solute entropy upon association $-T\Delta S$ (Wilson *et al.*, 1995). The free energy of binding difference $\Delta\Delta G_{\text{bind}}$ between wild-type and each c-Kit mutant and imatinib was calculated as

$$\Delta\Delta G_{\text{bind}} = \Delta G_{\text{bind}}(\text{wild-type}) - \Delta G_{\text{bind}}(\text{mutant}) \quad (4)$$

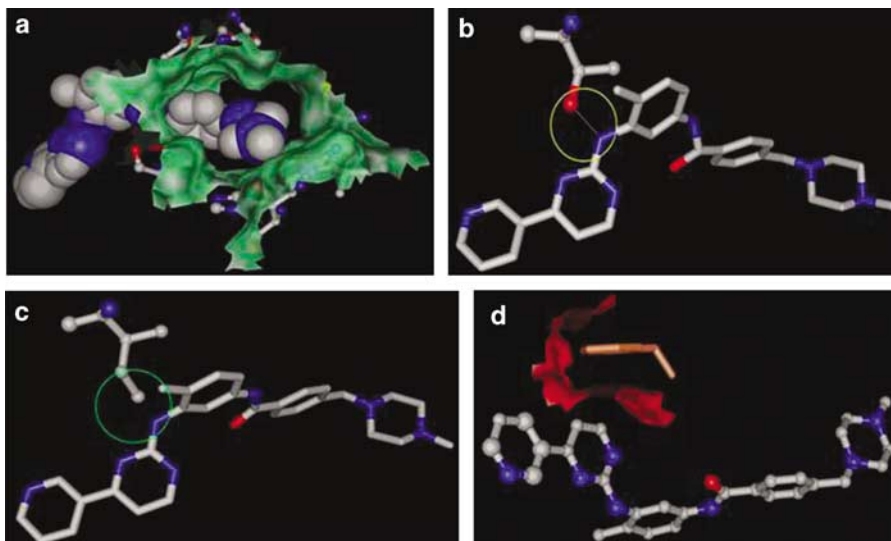
Accordingly, negative $\Delta\Delta G_{\text{bind}}$ values indicate highly unfavorable substitutions at the considered position, and *vice versa*. (a) Details of imatinib (atom-colored space-filling rendering) docked into the T670I c-Kit model showing the side chains of residues E640, V643, L644, C788, I789, H790, R791 and D810 (atom-colored stick-and-ball rendering). The green shadow, representing the amino-acid molecular surface, highlights the narrow space available to the inhibitor. (b) Comparison of the T670 and (c) I670 (both in atom-colored ball-and-stick rendering) interaction with imatinib (atom-colored stick rendering). (d) Steric clash (red surface) between imatinib (atom-colored ball-and-stick rendering) and F811 of the conserved DFG motif (light brown stick rendering).

reflects only in a slight alteration of some other imatinib contact points (E640, T670, C673 and F811) and some ATP-binding residues (K623 and E671). In particular, the readjustment of K623 results in a decreased interaction of this residue with E640 in C-helix (Figure 3e). Finally, V654 is engaged in two stabilizing hydrogen bond interactions. The former involves the C=O backbone group of V654 and the bridging water 956 on one side (ADL=2.85 Å), and the same water molecule and the C=O backbone group of G648 on the other (ADL=2.81 Å). The second H-bond involves the NH backbone moiety of V654 and the backbone C=O of I808, with an ADL of 3.03 Å. Interestingly, the same interactions are present in our MD trajectory of the A654 mutant, the former involving the same functional groups and water 1011 (ADL=2.90 and 2.83 Å, respectively), and the second being characterized by ADL=2.93 Å. As these H-bonds involve only backbone atoms of the residue at position 654, it is not surprising that the same two favorable interactions are preserved in our simulation of the A654 variant.

In this work, we report the biochemical characterization coupled with the molecular modeling of two *c-Kit* mutations, responsible for T670I and V654A substitutions, respectively, detected in three different patients with clinical and radiological symptoms of progressing disease during imatinib treatment. At disease onset, these patients displayed activating mutations affecting *c-Kit* exon 11 ($\Delta 557-558$, V559A and W557G, respectively), alterations associated to a significantly high response rate to imatinib (Corless *et al.*, 2004).

By treating transfected COS cells expressing mutated KIT receptors carrying these substitutions (KIT/T670I, KIT/ $\Delta 559$ /T670I, KIT/V654A and KIT/ $\Delta 559$ /V654A) with different doses of imatinib, we demonstrated that the presence of I (isoleucine) at position 670 or A (alanine) at position 654 is actually responsible for the acquired resistance to imatinib. For both the substitutions, in fact, the phosphorylation of the receptor persisted in the presence of 3 μM of the drug, indicating the occurrence of activated receptors. Interestingly, the

single and double mutant V654A appeared to be unphosphorylated and thus inhibited at 6 μM of imatinib, whereas the single and double mutant T670I did not. A reason for this behavior, at a molecular level, can be found in the results obtained from the MD simulations performed on the complex of imatinib with wild-type and both mutated KIT receptors. In fact, the values reported of the difference in the calculated free energies of binding of imatinib and the two mutant proteins clearly suggest that two different mechanisms should underline the lower inhibitor affinity. The $\Delta\Delta G_{\text{bind}}$ obtained for the KIT/T670I mutant is -3.84 kcal/mol, suggesting that the replacement of the polar residue T with the neutral I induces a substantial deformation of the binding pocket. Accordingly, the missing hydrogen bond between I670 and imatinib is not the only leading cause for drug binding failure to the protein. In utter analogy with what was observed by us for the homologous residue T315 in the *c-ABL* kinase domain (Pricl *et al.*, 2005), this failure instead results from a domino effect induced by the conformational readjustment necessary to accommodate the mutant residue, which involves several other important drug contact points. On the contrary, the smaller $\Delta\Delta G_{\text{bind}}$ value obtained for the V654A mutant is in line with a replacement of a hydrophobic residue into another of smaller size. A vast amount of structural data on various mutant proteins from different groups (Matthews, 1993; Buckle *et al.*, 1996; Dwyer *et al.*, 2000; Takano *et al.*, 2001) suggests that single-site amino-acid substitutions, especially in the case of conservative replacements, do not affect the global structure of proteins. In other words, mutant proteins usually retain overall structures that are very similar to those of their wild-type counterparts. In some cases, there are no conformational alterations, and the structure remains completely unchanged. In the rest of the cavity-creating variants, there are some movements in the position of atoms leaning the newly created cavity, but in each case the cavity remained in the structure of the variant. Clearly, this is the case of the KIT/V654A mutant: in this



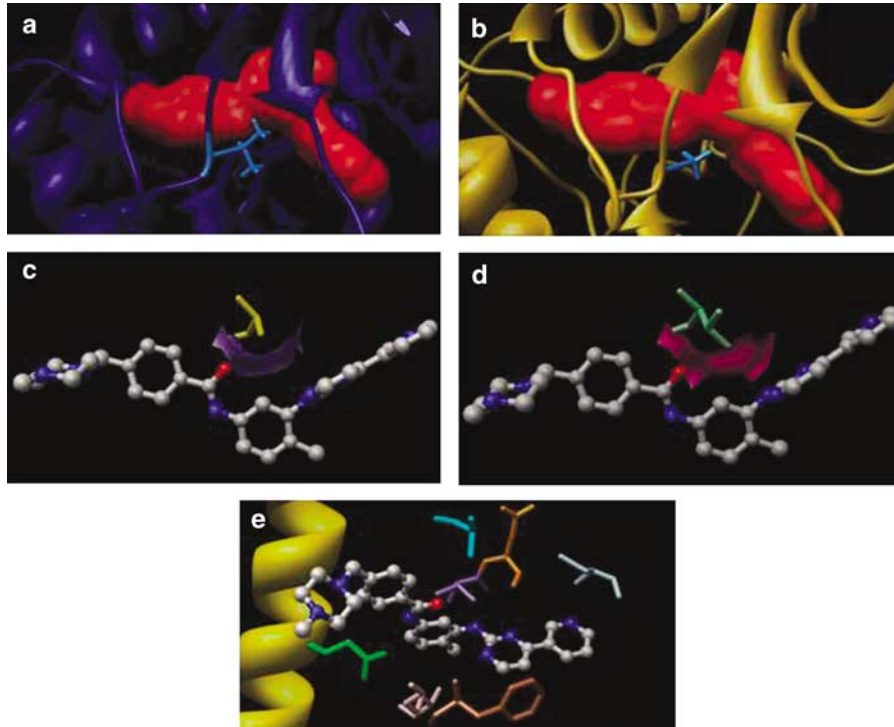


Figure 3 Molecular modeling of KIT/V654A mutant. (a) Ribbon traces (dark blue) of the backbone conformation of V654 c-Kit, with imatinib docked (molecular surface area in red) and V654 highlighted in light blue stick rendering. (b) Ribbon traces (gold) of the backbone conformation of A654 c-Kit, with imatinib docked (molecular surface area in red) and A654 highlighted in light blue stick rendering. (c) Surface complementarity (magenta) between V654 (green stick rendering) and imatinib (atom-colored stick-and-ball rendering). (d) Surface complementarity (purple) between V654 (gold stick rendering) and imatinib (atom-colored stick-and-ball rendering). (e) Details of the interaction of A654 and some imatinib contact points and ATP-binding residues. All residues are in stick rendering (color code: K623, pink; E640, green; A654, cyan; T670, purple; E671, orange; and C673, light blue). Imatinib is in atom-colored stick-and-ball rendering. C-helix is in gold ribbon rendering.

scenario, a ‘cavity-creating’ amino-acid substitution ($V \rightarrow A$) at a largely buried site such as position 654 in KIT does not lead to dramatic structural changes that completely alter or eliminate the cavity, but has an effect only on the structure in the vicinity of the substitution site.

All these observations are in line with our experimental evidences. Interestingly, the V654A mutation was detected in a patient treated with 400 mg/die of imatinib. It would have been appealing to observe the clinical and radiological evolution of this tumor if the patient would have been treated with imatinib at 800 mg/die. Based on our data, in fact, the effect of this mutation might be subverted by a dose escalation of the inhibitor and it would be expected to recapture a clinical response.

Another intriguing aspect that is becoming evident also in the literature (Chen *et al.*, 2004; Tamborini *et al.*, 2004, 2005; Debiec-Rychter *et al.*, 2005; Antonescu *et al.*, 2005; Wardelmann *et al.*, 2005) is why these mutations, T670I and V654A, are detected only in GIST patients who underwent imatinib treatment, whereas others, D820Y and N822K, are not (Debiec-Rychter *et al.*, 2005). Most likely, the frequency of these mutations is very low and only the selective pressure of the drug is able to make evident the resistant clones.

Surprisingly but perhaps not unexpected, most of the substitutions described affecting KIT receptor are

homologous to those described in ABL kinase of chronic myelogenous leukemia (CML) patients. In particular, T670I is homologous to T315I of BCR-ABL detected in some CML patients resistant to imatinib (Deininger *et al.*, 2005). As they affect the ATP pocket of the kinases, it could be supposed that other molecules could be employed as alternative drugs in a second-line therapy in both the diseases, GIST and CML. An example is represented by two new molecules, AMN107 (Novartis Pharmaceuticals, Basel, Switzerland) and BMS-354825 (Bristol Myers Squibb, New York, NY, USA), which are more effective than imatinib in a series of ABL mutants (O’Hare *et al.*, 2005).

In this light, biochemical analysis on mutated receptors testing the actual imatinib resistance coupled with molecular modeling could be of help in the design of new drugs and this combined approach will give important information to medical oncologist indicating the most suitable dose for escaping secondary resistance.

Acknowledgements

This work was supported by the following grants: AIRC (Associazione Italiana per la Ricerca sul Cancro) to Dr Pilotti and Dr Tamborini, and ‘Ministero della Sanita’, Ricerca Finalizzata 2004 Italy’.

References

- Antonescu CR, Besmer P, Guo T, Arkun K, Hom G, Koryotowski B et al (2005). *Clin Cancer Res* **11**: 4182–4190.
- Berendsen HJC, Postma JPM, van Gunsteren WF. (1984). *J Chem Phys* **81**: 3684–3690.
- Buckle AM, Cramer P, Fersht AR. (1996). *Biochemistry* **35**: 4298–4305.
- Case DA, Pearlman DA, Caldwell JD. (2000). *AMBER 7*. University of California: San Francisco, CA, USA.
- Chen LL, Trent JC, Wu EF, Fuller GN, Ramdas L, Zhang W et al. (2004). *Cancer Res* **64**: 5913–5919.
- Corless CL, Fletcher JA, Heinrich MC. (2004). *J Clin Oncol* **22**: 3813–3825.
- Corless CL, McGreevey L, Haley A, Town A, Heinrich MC. (2002). *Am J Pathol* **160**: 1567–1572.
- Cornell WD, Cieplak P, Bayly CI. (1995). *J Am Chem Soc* **117**: 5179–5197.
- Debiec-Rychter M, Cools J, Dumez H, Sciot R, Stul M, Mentens N et al. (2005). *Gastroenterology* **128**: 270–279.
- Deininger M, Buchdunger E, Druker BJ. (2005). *Blood* **105**: 2640–2653.
- Dwyer JJ, Gittis AG, Karp DA, Lattman EE, Spencer DS, Stites WE et al. (2000). *Biophys J* **79**: 1610–1620.
- Eriksson AE, Baase WA, Zhang XJ, Heinz DW, Blaber M, Baldwin EP et al. (1992). *Science* **255**: 178–183.
- Gilson MK, Sharp KA, Honig B. (1987). *J Comput Chem* **9**: 327–335.
- Heinrich MC, Corless CL, Demetri GD, Blanke CD, von Mehren M, Joensuu H et al. (2003). *J Clin Oncol* **21**: 4342–4349.
- Jorgensen WL, Chandrasekhar J, Buckner JK, Madura JD. (1983). *J Chem Phys* **79**: 926–935.
- Kellis Jr JT, Nyberg K, Sali D, Fersht AR. (1988). *Nature* **333**: 784–786.
- Lazaridis T, Archontis G, Karplus M. (1995). *Adv Protein Chem* **47**: 231–306.
- Lee B. (1993). *Protein Sci* **2**: 733–738.
- Loladze VV, Ermolenko DN, Makhatadze GI. (2002). *J Mol Biol* **320**: 343–357.
- Matthews BW. (1993). *Annu Rev Biochem* **62**: 139–160.
- Mol CD, Dougan DR, Schneider TR, Skene RJ, Kraus ML, Scheibe DN et al. (2004). *J Biol Chem* **23**: 31655–31663.
- Mol CD, Lim KB, Sridhar V, Zou H, Chien EY, Sang BC et al. (2003). *J Biol Chem* **278**: 31461–31464.
- Nicholls A, Sharp KA, Honig B. (1991). *Proteins: Struct Funct Genet* **11**: 281–296.
- O'Hare T, Walters DK, Stoffregen EP, Jia T, Manley PW, Mestan J et al. (2005). *Cancer Res* **65**: 4500–4505.
- Pace CN, Shirley BA, McNutt M, Gajiwala K. (1996). *FASEB J* **10**: 75–83.
- Pril S, Fermeglia M, Ferrone M, Tamborini E. (2005). *Mol Cancer Ther* **4**: 1167–1174.
- Reyes CM, Kollman PA. (2000). *J Mol Biol* **295**: 1–6.
- Ryckaert JP, Ciccotti G, Berendsen HJC. (1977). *J Comp Phys* **23**: 327–341.
- Sanner MF, Olson AJ, Spehner JC. (1996). *Biopolymers* **38**: 305–320.
- Srinivasan J, Cheatham III TE, Cieplak P. (1998). *J Am Chem Soc* **120**: 9401–9409.
- Takano K, Yamagata Y, Yutani K. (2001). *Biochemistry* **40**: 4853–4858.
- Tamborini E, Bonadiman L, Greco A, Albertini V, Negri T, Gronchi A et al. (2004). *Gastroenterology* **127**: 294–299.
- Tamborini E, Gabanti E, Lagonigro MS, Negri T, Pilotti S, Pierotti MA et al. (2005). *Cancer Res* **65**: 1115.
- Wardelmann E, Thomas N, Merkelbach-Bruse S, Pauls K, Speidel N, Buttner R et al. (2005). *Lancet Oncol* **6**: 249–251.
- Wilson EB, Decius JC, Cross PC. (1995). *Molecular Vibrations*. McGraw-Hill: New York, NY.